JOURNAL OF APPLIED ELECTROCHEMISTRY 9 (1979) 351–359

Local study of wall to liquid mass transfer in fluidized and packed beds. I. Mass transfer in fluidized beds

D. HUTIN, A. STORCK

Laboratoire des Sciences du Génie Chimique CNRS–ENSIC, 1, rue Grandville 54 042 Nancy, France

Received 26 May 1978

This paper deals with the local influence of particles on mass and momentum transfer at a surface immersed in a liquid fluidized bed. The experimental distributions of mass-transfer coefficients and shear stresses along the surface appear to be similar and suggest large hydrodynamic perturbations near the leading edge of the diffusional boundary layer. It is shown that the fluidized bed behaves as a turbulent pseudo-fluid and that the Chilton–Colburn analogy, expressing the equivalence between mass and momentum transfer applies locally. The results of the study lead to a qualitative explanation of the influence of the fluidization parameters on the overall surface to liquid mass transfer coefficient in fluidized beds.

Nomenclature

a	coefficient in Equation 6
D	molecular diffusion coefficient
d_p	particle diameter
d	microelectrode diameter
j_M	$= k/(u/\epsilon)(Sc)^{2/3}$ Colburn j-factor
k	local mass transfer coefficient
k'	local mass transfer coefficient defined by Equation 1
k'_C	k' mass transfer coefficient given by the Chilton–Colburn analogy
$\bar{k}$	overall mass transfer coefficient
L	length of the transfer surface
m, n, p	exponents in Equations 6 and 7
s	$= (\partial V_x/\partial y)_{y=0}$ velocity gradient at the transfer surface
(Sc)	$= \nu/D$ Schmidt number
u	liquid superficial velocity
u_{max}	maximum fluidization velocity
V_x	length velocity
x	length coordinate
x_0	length of the inactive part of electrode
y	normal coordinate
ϵ	bed porosity
ϵ_{max}	porosity corresponding to the maximum of k in a fluidized bed
ρ_F	fluid density
ρ_S	particle density
η	dynamic viscosity
ν	kinematic viscosity
τ	$= \eta s$ shear stress at the wall

1. Introduction

The study of mass transfer between a flowing liquid and a solid boundary immersed in fluidized beds of inert particles has been the subject of extensive experimental and theoretical works and the use of fluidized beds has even been suggested for electrolysis operations [1].

Some recent papers [2, 3] have reviewed the overall influence of geometrical and hydrodynamic parameters on wall to liquid mass transfer.

According to these studies, it appears that: (a) a homogeneous fluidized bed can be considered as an intermediate state between the fixed bed and the empty tube (without particles), (b) the continuous agitation of fluidized particles is not responsible for the observed high mass transfer rates and the particles only act as turbulence promoters of the fluid in the same way as if they were fixed in their mean statistical positions [3], and (c) due to the hydrodynamic complexity of fluidized beds, only semi-empirical correlations were proposed for representing the experimental mass transfer results.

Most previous studies (except [2, 4]) have examined the macroscopic behaviour by measuring the overall mass transfer rates on obstacles larger than the fluidized particles. Consequently, several points remain to be elucidated, for example:

(a) Why does the overall mass transfer decrease with increasing length L of the transfer surface in the flow direction?

(b) What are the relationships between mass and momentum transfer in fluidized beds?

Clearly a better understanding of the transfer mechanisms can only be obtained with more refined local measurements.

The present paper aims at obtaining local quantitative information on mass transfer coefficients and fluid shear stresses along a transfer surface, thus answering those questions. The relationship between local mass and momentum transfer is also investigated.

2. Experimental

2.1. *Hydraulic apparatus*

The equipment (Fig. 1) is the same as described in previous papers [5, 6].

The liquid stocked in a thermostated tank (30° C), flows through a calming section of spherical glass beads, through an 'Altuglas' column with an internal diameter of 92 mm and returns by gravity to the tank.

Fluidization flow rates are measured with a calibrated diaphragm.

2.2. *Determination of the transfer coefficients*

As in previous studies [3, 5, 6], the overall and local wall to liquid mass transfer coefficients were obtained electrochemically by means of the cathodic reduction of ferricyanide. The liquid (electrolyte) is an equimolar mixture (0·005 M) of potassium ferrocyanide and ferricyanide in a supporting electrolyte of NaOH (0·5 M).

The true ferricyanide concentration is determined by amperometric titration on a rotating disc electrode.

Experimental values obtained at a constant temperature (30° C) for the electrolyte kinematic viscosity ν, the ferricyanide diffusion coefficient D and the Schmidt number (Sc) are $0{\cdot}914 \times 10^{-2}$ $cm^2 s^{-1}$, $8{\cdot}8 \times 10^{-6} cm^2 s^{-1}$ and 1040, respectively.

2.3. *Electrodes*

The anode is a large sheet of nickel flush fitted on the fluidization tube.

The working electrode (Fig. 1) is cylindrical and is immersed along the fluidization column axis. It consists of a 3·25 cm long PVC tip, a nickel cylinder (length $L = 13{\cdot}8$ cm, diameter 1·5 cm) plated with gold and platinum successively, and a row of 12 (diameter 0·55 mm) platinum microelectrodes.

Each microelectrode is insulated from the conducting cylinder by a film of Araldite of very small thickness (cf. Fig. 1). The working electrode incorporated in a classical three electrode potentiostatic circuit allows the determination of three important experimental parameters [7]:

(a) the overall mass transfer coefficient $\bar{k}$ between the transfer surface and the flowing liquid.

(b) the local mass transfer coefficient k in a given position (by measuring the current generated at the microelectrode, the cylindrical electrode being electrically connected).

(c) the fluid local velocity gradient at the wall

$$s = \left(\frac{\partial V_x}{\partial y}\right)_{y=0}.$$

Indeed [8], under such conditions, the mass-transfer coefficient k' through the incipient diffusional boundary layer on a microelectrode can be related to s by the expression

$$k' = 0{\cdot}807 \frac{D^{2/3} s^{1/3}}{d^{1/3}} \qquad (1)$$

where d is the microelectrode diameter.

This relation, frequently used in fluid mechanics, is valid for pure liquids in laminar and turbulent flow.

It has been shown previously [9] that the thickness of the concentration zone on a microelectrode was much smaller than that of the viscous sublayer.

We supposed that the addition of particles to the liquid does not modify the validity of Equation 1 and that a time-average local velocity gradient at the wall can be calculated.

According to this hypothesis, the fluidized particles only act as turbulence promoters of the liquid phase, which is in good agreement with previous results [3].

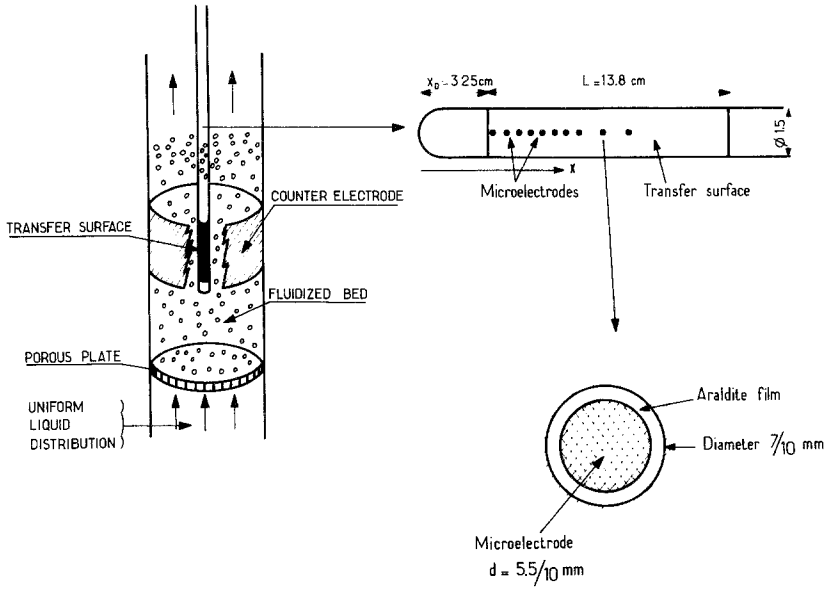

Fig. 1. Schematic view of the hydraulic apparatus and the transfer surface.

3. Results

3.1. *Empty tube*

At two different liquid flow rates u, Figs. 2 and 3 show the experimental variations of k and k' with the position along the transfer surface.

A general decrease of these two coefficients can be observed, corresponding to the development of the hydrodynamic and diffusional boundary layers along the wall.

In the particular case when the cylindrical electrode can be approximated to a flat plate (high curvature radius), the local mass transfer coefficient along the wall is given by [10]

$$k = 0{\cdot}332D(Sc)^{1/3}\left(\frac{u}{\nu x}\right)^{1/2}\left[1-\left(\frac{x_0}{x}\right)^{3/4}\right]^{-1/3} \tag{2}$$

where x_0 is the distance between the leading edges of the hydrodynamic and diffusional boundary layers.

Integration of this expression between $x = x_0$ and $x = x_0 + L$ leads to the overall mass transfer coefficient $\bar{k}$ between wall and liquid

$$\bar{k} = 0{\cdot}664D(Sc)^{1/3}\left(\frac{u}{\nu L}\right)^{1/2}\left[\left(1+\frac{x_0}{L}\right)^{3/4}-\left(\frac{x_0}{L}\right)^{3/4}\right]^{1/3}.$$

In the same way the local velocity gradient s on the plate is related to the liquid flow rate u by

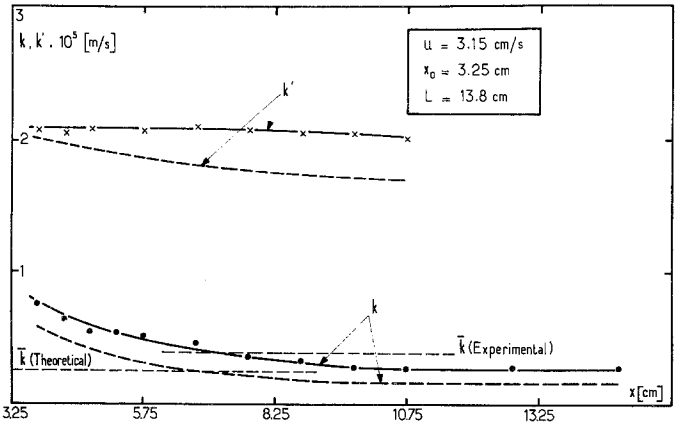

Fig. 2. Experimental and theoretical variations of k and k' without particles (empty tube: $u = 3{\cdot}15$ cm s^{-1}).

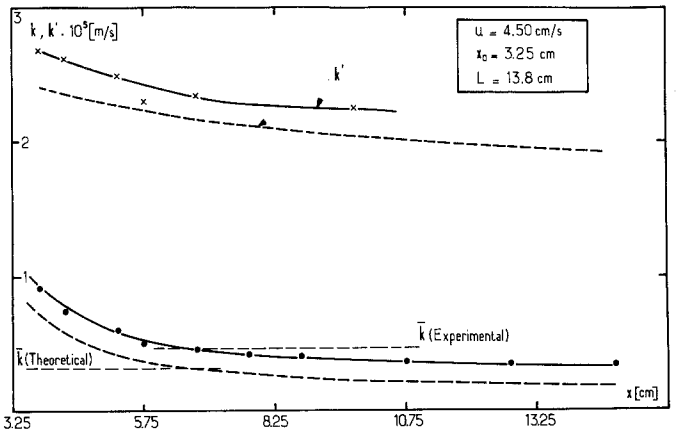

Fig. 3. Experimental and theoretical variations of k and k' without particles ($u = 4{\cdot}50$ cm s^{-1}).

$$s = 0{\cdot}332 \frac{u^{3/2}}{\nu^{1/2} x^{1/2}}. \qquad (3)$$

The theoretical values of s deduced from Equation 3 allow the coefficients k' to be calculated through Equation 1.

The theoretical variations of k and k' with the position along the wall, calculated from Equations 2 and 3 are reported on Figs. 2 and 3 and compared to experimental values obtained by the microelectrode technique. As seen, the agreement between experiment and theory is satisfactory and confirms the increase in thickness of the diffusional and hydrodynamic boundary layers. One should note, however, that in the two sets of results the experimental values are larger than those predicted from theory.

This deviation may be explained by the difficulty in measuring the true microelectrode surface area with good precision and in obtaining a homogeneously fluidized bed as well as uniform liquid distribution at the bed inlet.

The observed deviations are however, small enough to demonstrate the validity of the local measurements. As a result the experimental technique may be applied to fluidized beds.

3.2. *Fluidized beds*

Figs. 4–6 show the variations of k and k' along a transfer surface immersed in a fluidized bed of spherical glass particles ($\rho_S = 2{\cdot}54$ g cm^{-3}). The superficial liquid velocity u (and consequently the bed porosity ϵ) is different for the three runs.

From these figures, the following remarks can be made: the variations of k and k' with the position are quite symmetrical, which shows the analogy between mass and momentum transfer; the coefficients k and k' have very different values; the mass transfer rates to microelectrodes in an inert wall are always much larger than those obtained with the conducting wall; near the leading edge of the diffusional boundary layer, k and k' show unstable values with an oscillatory form around a mean value.

These curious experimental oscillations could be explained by one or several of the following points:

(a) The microelectrode surface area is not measured with good precision and the uncertainty on this parameter is the cause of the observed phenomenon.

(b) The hydrodynamic flow regime is not uniform in the fluidization column.

(c) The presence of the transfer surface in the fluidized bed causes hydrodynamic perturbations near the leading edge of the electrode, the perturbations becoming progressively smaller and smaller along the wall.

The two first assumptions have to be rejected because otherwise the same perturbations should have been observed in the empty tube (Figs. 2 and 3). Consequently the last hypothesis seems to be the more reasonable to explain the local instability of the observed oscillations. In the next paragraph an important consequence of this observation will be discussed.

The influence of the superficial liquid velocity u on k and k' is shown in Figs. 7 and 8, which present the variations of k, $\bar{k}$ and k' with the mean bed porosity ϵ for different positions on the wall

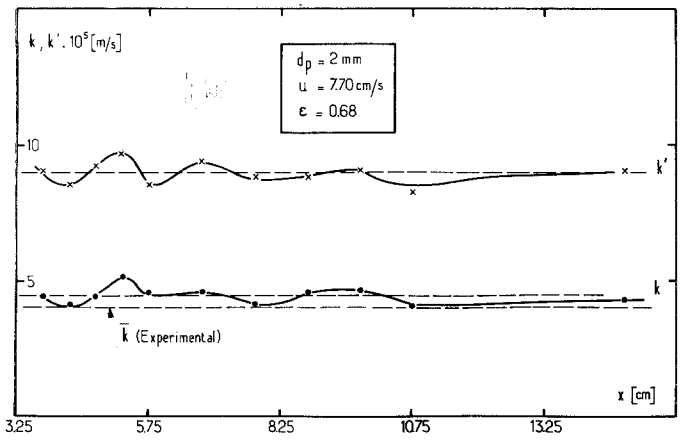

Fig. 4. Variations of k and k' with position along the transfer surface immersed in a fluidized bed ($d_p = 2$ mm; $u = 7{\cdot}70$ cm s^{-1}; $\epsilon = 0{\cdot}68$).

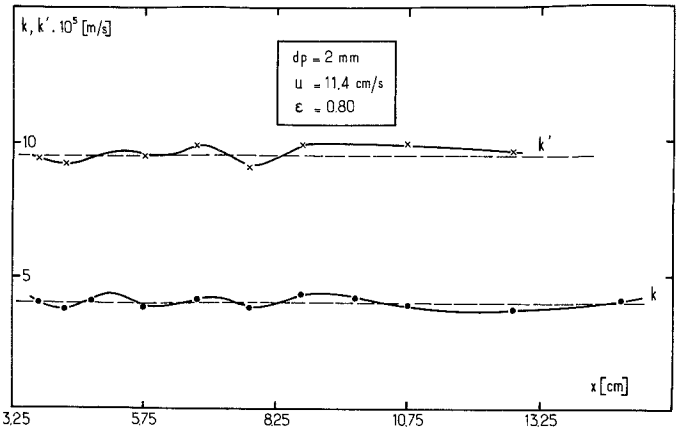

Fig. 5. Variations of k and k' with position along the transfer surface ($d_p = 2$ mm; $u = 11{\cdot}4$ cm s^{-1}; $\epsilon = 0{\cdot}80$).

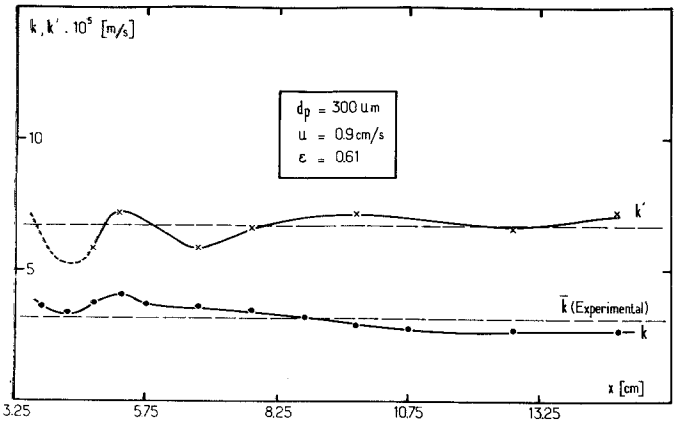

Fig. 6. Variations of k and k' with position for $d_p = 0{\cdot}3$ mm; $u = 0{\cdot}9$ cm s^{-1} and $\epsilon = 0{\cdot}6$.

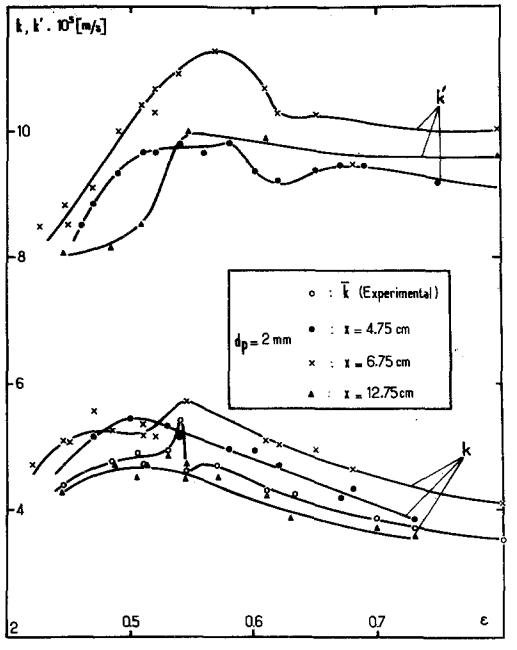

Fig. 7. Experimental variations of k, k' and $\bar{k}$ with porosity ϵ for different positions along the transfer surface ($d_p = 2$ mm).

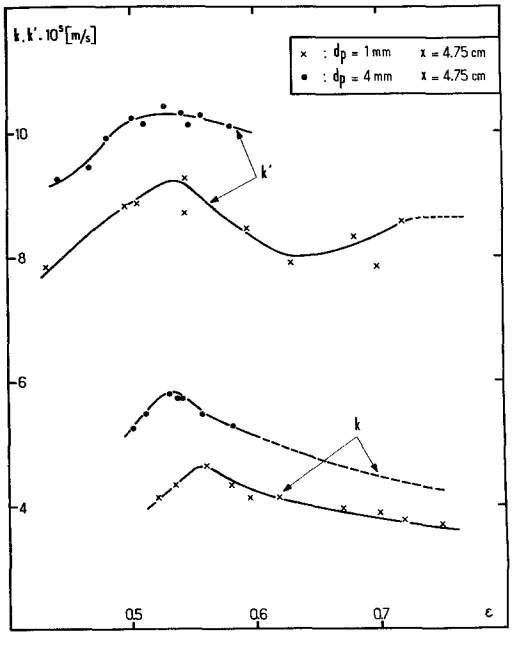

Fig. 8. Experimental variations of k and k' with porosity ϵ for two different particle diameters.

and for three particle diameters d_p. The corresponding results are in good agreement with the observed macroscopic influence of the hydrodynamic and geometrical parameters [5, 6].

(a) the coefficients k, $\bar{k}$ and k' vary with the bed porosity and are maximum for ϵ between 0·5–0·6. The curve $\bar{k}$ versus ϵ has an intermediate position with respect to the local k values.

(b) at a given ϵ value, k and k' increase with increasing particle diameter d_p (Fig. 8), the maximum of transfer being displaced towards smaller porosities.

(c) the curves corresponding to k' present an anomaly around a porosity of 0·62 : k' first increases with the porosity, passes through a maximum value then decreases and seems to reach a minimum value. This anomaly cannot be explained simply, but has already been observed by Coeuret [11] in a study relative to mass transfer during the impact of impinging jets on small surfaces. Hydrodynamic phenomena have been proposed to account for such findings [11].

4. Discussion

4.1. *Chilton–Colburn analogy at the microscopic scale*

Let us assume that the liquid containing the fluidized particles behaves as a turbulent pseudo-phase exchanging mass with the wall and that the interstitial fluid velocity u/ϵ is the determining parameter. This analogy between a homogeneous fluidized bed and a pseudo-fluid has been previously made by different authors such as Furukawa and Ohmae, and Schugerl [12, 13].

For turbulent heat and mass transport processes in pure liquids, Thomas and Fan [14] have proposed a transport model based on the principle of surface renewal and have shown that the familiar Colburn analogy [15] applies.

In order to confirm the validity of this hypothesis (approximation of the fluidized bed to a turbulent pseudo-phase), which makes an equivalence between mass and momentum transfer, we write the equation

$$j_M = \frac{k}{u/\epsilon}(Sc)^{2/3} = \frac{\tau}{\rho_F (u/\epsilon)^2}$$

where τ is the local shear stress of the pseudo-

fluid containing the particles. This equation allows τ to be expressed as a function of the local mass transfer coefficient k:

$$\tau = \rho_F (Sc)^{2/3} k \frac{u}{\epsilon}. \qquad (4)$$

Similarly the k'_C coefficient corresponding to the local applicability of the Chilton–Colburn analogy, is related to k as

$$k'_C = 0{\cdot}807 \frac{D^{2/3}\tau^{1/3}}{\eta^{1/3} d^{1/3}}$$

$$= 0{\cdot}807 \frac{D^{1/3}(Sc)^{-1/9}}{d^{1/3}} \left(k\frac{u}{\epsilon}\right)^{1/3}. \qquad (5)$$

The k'_C values can then be obtained from the experimental values of k (results of Figs. 7 and 8) and compared to the k' values deduced from the measurements on an inert wall.

This comparison has been made on Fig. 9, which presents the variations of the ratio k'_C/k' with ϵ for three particle diameters. As seen, this ratio is between 0·75–1 except at small porosities. In Figs. 2 and 3, we found that experimental values of k and k' in the empty tube are always larger than the values predicted from theory. Due to similar uncertainties, the true value of k' in a fluidized bed may also be smaller than the experimentally determined k' value, which would result in a ratio k'_C/k' close to unity.

Consequently, experimental results confirm,

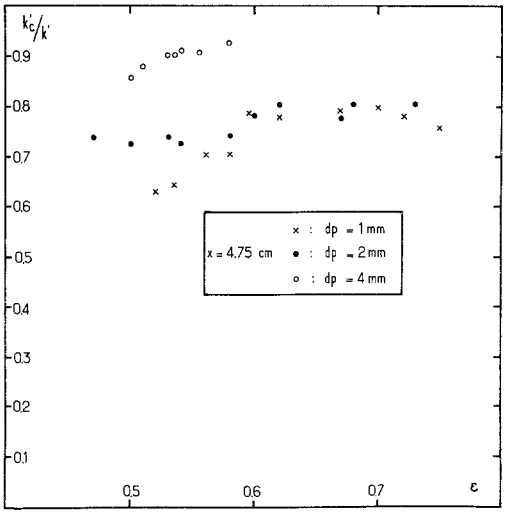

Fig. 9. Verification of the local applicability of the Chilton–Colburn analogy: variations of k'_C/k' with bed porosity.

within experimental precision, that a fluidized bed behaves as a turbulent pseudo-phase and that, according to a previous study [3], the particles only act as turbulence promoters of the liquid.

4.2. *Consequence of the analogy's applicability. Influence of the fluidization parameters*

The fluid shear stress τ or the dissipated energy per unit volume in unit time in the vicinity of the solid boundary, τ^2/η, depends on three parameters: the physical properties of the liquid, the superficial fluid velocity u, and the particle concentration in the liquid phase, $(1-\epsilon)$.

$$\tau = F|\text{fluid properties}, u, (1-\epsilon)|.$$

In a small domain of variations, τ can be expressed as

$$\tau = a u^m (1-\epsilon)^p \quad (m > 1) \qquad (6)$$

the parameter a including the contribution due to the physical properties of the liquid and the two exponents m and p being positive

Furthermore the expansion law of Richardson and Zaki [16]

$$u/u_{max} = \epsilon^n \qquad (7)$$

(u_{max} being the maximum fluidization velocity) allows the flow rate u corresponding to the porosity ϵ to be calculated. Combining Equations 4, 6 and 7 leads to the following expression for the local mass transfer coefficient k:

$$k = \frac{a u_{max}^{m-1}}{\rho_F (Sc)^{2/3}} \epsilon^{n(m-1)+1}(1-\epsilon)^p. \qquad (8)$$

These mathematical developments lead to a qualitative explanation of the influence of the fluidization parameters on the wall to liquid mass transfer coefficient

4.2.1. Maximum value of the mass transfer coefficient. We bear in mind that k or $\bar{k}$ present a maximum value when the bed porosity ϵ is between 0·5–0·6 [5, 6]. Differentiating Equation 8 with respect to ϵ, one easily shows that a maximum of k occurs for the following value ϵ_{max} of the porosity:

$$\epsilon_{max} = \left[1 + \frac{p}{n(m-1)+1}\right]^{-1}. \qquad (9)$$

For spherical particles, the exponent n of the expansion law is 4·6 in the Stokes regime and 2·4 in the Newton regime. In view of the dimensions

and density of the particles, n is close to 2·4. Moreover by analogy with the mean shear stresses on particles in an expanded fixed bed [3], the exponent m in Equation 6 is approximately 1 or 2 depending on the flow regime (laminar or turbulent).

The values of the parameters n and m and the porosity ϵ_{max} are summarized in Table 1 for different values of p. The porosities corresponding to the maximum transfer rates are found to be in good agreement with the experimental values [5, 6] ($0{\cdot}5 < \epsilon_{max} < 0{\cdot}6$).

It has to be noted also that in most fluidized beds, the real operating conditions correspond to those on the third line of Table 1 whereas the values on the first line are rarely valid.

4.2.2. Influence of particle diameter d_p and density ρ_S. Concerning the influence of these two parameters, Equation 8 combined with the expression for u_{max} in the Newton regime (most frequent case)

$$u_{max} = \left[3gd_p\frac{(\rho_S - \rho_F)}{\rho_F}\right]^{1/2}$$

shows that at a given ϵ value k increases with particle diameter d_p (increase in $d_p^{[(m-1)/2]}$) and k increases with the difference $(\rho_S - \rho_F)$ [increase in $(\rho_S - \rho_F)^{[(m-1)/2]}$].

For the conditions of the third line in Table 1, these results are found to be in good agreement with the influence of these parameters observed previously [5, 6] and confirm the validity of the preceding developments.

Table 1. Influence of the flow regime on the porosity ϵ_{max} for different values of the parameter p

	ϵ_{max}			
Flow regime	$p=1$	$p=2$	$p=3$	$p=4$
laminar flow regime $n = 4{\cdot}6$ $m = 1$	0·50	0·33	0·25	0·20
turbulent flow regime $n = 2{\cdot}4$ $m = 2$	0·77	0·63	0·53	0·46
intermediate flow regime $n = 2{\cdot}4$ $m \simeq 1{\cdot}5$	0·68	0·61	0·42	0·35

4.3. *Transfer mechanism*

In most work concerning overall mass transfer in fluidized beds, the length of the transfer surface in the flow direction was found to have a similar influence to that observed in the empty tube ($\epsilon = 1$): at a given ϵ value, the mass transfer rate to the wall decreases with increasing L.

In view of the lack of information on the microscopic scale, most of the authors have assumed that a laminar liquid film of increasing thickness exists along the transfer surface.

The local experimental results presented in this work are not in agreement with this concept. In fact, the surface would consist of two different zones. The first corresponding to the leading edge of the electrode is characterized by large hydrodynamic instabilities becoming smaller and smaller along the electrode and leading to higher mass transfer rates. The second zone located upstream is characterized by a quasi-uniformity of the mass transfer coefficients. Therefore, except at the leading edge of the wall, the boundary layer thickness would be constant and present small oscillatory deviations around a mean value.

These results could be perhaps compared to those of a recent study [17] concerning the oscillatory form of the vertical particle velocity distribution in liquid fluidized beds. However, experimental observations of the dynamics of particle movement near the transferring wall would be necessary to explain more precisely the observed phenomena.

5. Conclusions

The microelectrode technique in an inert or conducting surface appears to be a new tool in the understanding of the transfer mechanisms to surfaces immersed in homogeneous fluidized beds.

For the empty tube (without particles), the theory of the laminar boundary layer along a flat plate has been successfully verified and confirms the validity of the local measurements.

In a fluidized bed, the study on the influence of the position along the transfer surface shows

the existence of a hydrodynamic disturbed region followed by a second zone with a quasi-uniformity of the transfer rates.

The experimental results also demonstrate that the fluidized bed behaves as a turbulent pseudo-phase, for which the well-known Chilton–Colburn analogy applies satisfactorily. Important consequences concerning the influence of the fluidization parameters have been deduced. The continuous agitation of particles has sometimes been considered responsible for the good transport properties in fluidized beds.

This local study of mass and momentum transfer shows that the particles act as turbulence promoters of the liquid and confirms therefore the results of a recent study [3].

References

[1] F. Coeuret, P. Le Goff and F. Vergnes, French Patent 1500 269 (1967).
[2] H. A. Xifra and U. Böhm, *Lat. Amer. J. Chem. Eng. Appl. Chem.* **5** (1975) 39.
[3] A. Storck and F. Coeuret, *Canad. J. Chem. Eng.* **55** (1977) 427.
[4] J. W. Smith and D. H. King, *Canad. J. Chem. Eng.* **53** (1975) 41.
[5] A. Storck, F. Vergnes and P. Le Goff, *Powder Technol.* **12** (1975) 215.
[6] A. Storck and F. Vergnes, *ibid* **12** (1975) 209.
[7] A. Storck and F. Coeuret, *Electrochim. Acta* **22** (1977) 1155.
[8] L. P. Reiss and J. J. Hanratty, *Amer. Int. Chem. Engineers J.* **9** (1963) 154.
[9] M. Labbe, Thesis, Nancy (1975).
[10] F. Coeuret and F. Vergnes, *C.R. Acad. Sci., Paris* **273c** (1971) 580.
[11] F. Coeuret, *Chem. Eng. Sci.* **30** (1975) 1257.
[12] J. Furukawa and T Ohmae, *Ind. Eng. Chem.* **50** (1950) 821.
[13] K. Schugerl, M. Herz and F. Fetting, *Chem. Eng. Sci.* **15** (1961) 1.
[14] L. C. Thomas and L. T. Fan, *Israel J. Technol.* **8** (1970) 439.
[15] T. H. Chilton and A. P. Colburn, *Ind. Eng. Chem.* **26** (1934) 1183.
[16] J. F. Richardson and W. N. Zaki, *Trans. Inst. Chem. Eng.* **32** (1954) 35.
[17] A. Kmiec, *Chem. Eng. J.* **15** (1978) 1.